Available online at www.sciencedirect.com
SCIENCE DIRECT
Catalysis Today 107–108 (2005) 362–370
CATALYSIS TODAY
www.elsevier.com/locate/cattod

From homogeneous to heterogeneous catalysis: Supported Pd(II) metal complexes with chiral triaza donor ligands Comparative catalytic study with Rh(I) and Ir(I) complexes for hydrogenation reactions

Camino González-Arellano [a,c], Avelino Corma [b], Marta Iglesias [a,**], Félix Sánchez [c,*]

[a] *Instituto de Ciencia de Materiales de Madrid, CSIC, Cantoblanco, 28049 Madrid, Spain*
[b] *Instituto de Tecnología Química, UPV-CSIC, Avda de los Naranjos s/n 46022, Valencia, Spain*
[c] *Instituto de Química Orgánica, CSIC, Juan de la Cierva 3, 28006 Madrid, Spain*

Available online 18 August 2005

Abstract

Palladium complexes with the chiral triaza ligands *N,N′*-bis{[(*S*)-(1-benzylpyrrolidin-2-yl)]methyl}amine and *N,N′*-bis{[(*S*)-(1-benzylpyrrolidin-2-yl)]methyl}-*N*-propylamine have been obtained. The fixation of the preformed palladium complex, {[Pd(*N,N′*-bis{[(*S*)-(1-benzylpyrrolidin-2-yl)]methyl}-*N*-[3-(triethoxysilyl)propyl]amine)(cod)]PF_6}, on mesostructured silicates and delaminated zeolites (silica, MCM-41, ITQ-2 and ITQ-6) and their use, under heterogeneous conditions, for the hydrogenation reactions are reported. The catalytic activity and selectivity are higher to that observed under homogeneous conditions, as a consequence of the complex- and/or reagents-to-support interaction. The strength of stable covalent bond between support and supported complex allows the recovery and recycling of the supported catalysts for a number of cycles. Atomic absorption analysis of the reaction solutions shows that there is no metal leaching into the solutions. A comparative catalytic study with the respective Rh(I) and Ir(I) complexes for olefin hydrogenation reactions was also given.

Keywords: Palladium; Hydrogenation; Immobilisation; Mesoporous

1. Introduction

In 1994, Togni and Venanzi [1] reported very promising results with nitrogen donor ligands in asymmetric catalysis. Six years later, Fache et al. [2] published a precise review on the current state of the investigations in this area and recently, one revision [3] shows the progress accumulated since then in catalytic transformations using tetraaza ligands. Nitrogen-containing ligands have several distinct advantages. First, they are largely available in enantiomerically pure form, both in the chiral pool (quinine, cinchonine and sparteine) and as cheap industrial chemical intermediates. On the other hand, chirality on the nitrogen atom is difficult to obtain. Contrary to the phosphines, the chiral nitrogen atoms epimerize instantaneously at room temperature; the formation of a stable chiral centre on a nitrogen atom is however possible by using bicyclic structures.

The second advantage of the nitrogen-containing ligands lies in the chemistry of the nitrogen functional group itself. The chemistry of these is not always easy, but it has received such abundant attention that there exists, in most cases, numerous synthetic solutions to each possible transformation of these compounds. As a result, these synthetic possibilities allow tailor-made modifications for the preparation of ligands with specific physicochemical properties. In particular, the interactions with the transition metals may be widely varied by preparing X-type ligands (amides and sulfonamides), L-type ligands (amines) or π-type ligands (imines).

* Corresponding author. Tel.: +34 91 5622900; fax: +34 91 5644853.
** Corresponding author. Tel.: +34 91 3349000; fax: +34 91 3720623.
E-mail addresses: marta.iglesias@icmm.csic.es (M. Iglesias), felix-iqo@iqog.csic.es (F. Sánchez).

0920-5861/$ – see front matter
doi:10.1016/j.cattod.2005.07.096

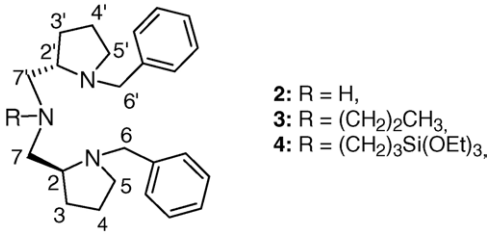

Fig. 1. Chiral triaza ligands.

Nitrogen-containing ligands are being used more and more in asymmetric catalysis. They turn out to be suitable for any type of catalysis and especially for heterogeneous catalysis [4–6], which is one of their main advantages over phosphines. In addition, nitrogen-containing ligands may be used in asymmetric catalysis with transition metals, which are less expensive than noble metals [7].

Starting from the readily available L-proline, our group [8–12] reported the preparation of the tetraaza C_2-symmetric ligands and their metal complexes (Rh(I), Ir(I), Cu(I) and Mn(II)). These complexes were tested on the asymmetric hydrogenation, cyclopropanation and oxidation reactions, showing that ligands gave only poor enantioselectivities (<20%) but excellent chemical yields (>85%). These catalysts have been heterogenised, and the strategy used preserve as much as possible the co-ordination sphere of the metal [13]. The heterogenised complexes are still more stable than their homogeneous counterpart and they can be used several times without decreasing activity. Nevertheless, the enantioselectivity achieved with the heterogeneous systems remains close to that obtained with the homogeneous ones.

Herein, we present a new family of Pd(II) complexes with chiral triaza ligands (Fig. 1) compared it with the respective Rh(I) and Ir(I) complexes and investigate their co-ordination chemistry and catalytic properties in detail, and how efficient and selective heterogeneous zeolite systems involving this type of ligands could be designed.

2. Experimental

2.1. General

Preparation of organometallic complexes was carried out under dinitrogen by conventional Schlenk-tube techniques. All solvents were carefully degassed before use. The silylating agent iodopropyltriethoxysilane was obtained by halogen change starting from the commercial chloropropyltriethoxysilane. C, H and N analyses were carried out by the analytical department of the Institute of Materials Science (CSIC). Metal contents were analysed by atomic absorption using a Perkin-Elmer AAnalyst 300 atomic absorption and plasma ICP Perkin-Elmer 40 spectrometers. Mass spectra were performed on a Hewlett-Packard 1100 MSD mass spectrometer (ESI-MS, APCI-MS) with positive mode. IR spectra were recorded on a Bruker IFS 66 V/s spectrophotometer (range 4000–200 cm^{-1}) in KBr pellets; ^1H, ^{13}C NMR spectra were taken on a Varian XR300 and a Bruker 200 spectrometers. ^1H NMR chemical shifts are given in ppm using tetramethylsilane as an internal standard. High resolution ^{13}C MAS or CP/MAS-NMR spectra of powdered samples, in some cases also with a Toss sequence, in order to eliminate the spinning side bands, were recorded at 100.63 MHz, 6 μs 90° pulse width, 2 ms contact time and 5–10 recycles delay, using a Bruker MSL 400 spectrometer equipped with an FT unit. The spinning frequency at the magic angle (54°44′) was 4 kHz. Optical rotation values were measured at the sodium-D line (589 nm) with a Perkin-Elmer 241 MC polarimeter. Gas chromatography analysis was performed using a Hewlett-Packard 5890 II with a flame ionisation detector in a cross-linked methylsilicone column [14]. The inorganic support for anchoring were a purely siliceous MCM-41 [15,16], delaminated zeolites ITQ-2 [17] and ITQ-6 [18–21] and SBA-15 [22]. The textural characteristics of the solids are given in Table 1. Ligands *N*,*N*-bis{[(*S*)-1-benzylpyrrolidin-2-yl]methyl}amine (**2**), *N*,*N*′-bis{[(2*S*)-(1-benzylpyrrolidinyl)]methyl}-*N*-propylamine (**3**) and *N*,*N*′-bis{[(2*S*)-(1-benzylpyrrolidinyl)]-methyl}-*N*-[3-(triethoxysilyl)propyl]amine (**4**) were prepared according to modified published methods [23,24]. Rhodium and iridium complexes were synthesised as we have described in Ref. [24].

2.2. Typical procedure for homogeneous palladium complexes

$AgPF_6$ (58 mg and 0.23 mmol) in dichloroethane (30 ml) was added to $[PdCl_2(cod)]$ (cod = cycloocta-1,5-diene) (65 mg and 0.23 mmol) in dichloroethane (10 ml) and the mixture was stirred vigorously at room temperature for 1 h. Precipitated silver chloride was filtered off and the yellow solution was treated with the ligand (0.23 mmol) in the same

Table 1
Textural characteristics of the solid supports

Support	Si/Al	BET surface area ($m^2\ g^{-1}$)	Micropore surface (*t*-plot $m^2\ g^{-1}$)	External (or mesoporous) suface area ($m^2\ g^{-1}$)
Silica	–	540	–	540
MCM-41	∞	1030	0	1030
ITQ-2	∞	830	130	700
ITQ-6	∞	618	10	608

solvent. The mixture was stirred for 12 h under reflux. The solvent was evaporated under reduced pressure to 2 ml. Careful addition of diethyl ether caused the precipitation of a solid, which was collected by filtration, washed with diethyl ether and dried under vacuum (10^{-3} mm Hg) to give the complex.

*2.2.1. [PdCl(**2**)] (Pd2A)*

Black. Yield: 10%. mp: 130–132 °C. Elemental analysis: (found: C: 58.8; H: 6.5; N: 8.1; Pd: 20.9%). Calcd. for $C_{24}H_{32}N_3Cl$ Pd (503.5): C: 57.1; H: 6.4; N: 8.3; Pd: 21.1. IR (KBr, cm^{-1}): ν = 457 (Pd–N); 326 (Pd–Cl). ^{1}H-RMN ($CDCl_3$, ppm): δ = 7.60–7.52 (4H, m, H_{arom}); 7.45–7.29 (6H, m, H_{arom}); 4.52, 4.17 (4H, d, AB, J = 12.9 Hz, CH_2Ph); 3.94–3.70 (4H, m, 2$H_{7,7'}$); 3.57–3.37 (4H, m, $H_{2,2''}$, 2H_5); 3.02–2.93 (2H, m, 2$H_{5'}$); 2.16–2.05 (4H, m, 2H_4, 2H_3); 1.98–1.82 (4H, m, 2$H_{3'}$, 2$H_{4'}$). ^{13}C-RMN ($CDCl_3$, ppm): δ = 131.38, 130.44, 129.64 (C_{arom}); 68.90 (C_2); 61.47 (C_7); 60.03 (CH_2Ph); 54.20 (C_5); 26.52 (C_4); 23.50 (C_3). EM (*m*/*z*): 504 ([Pd(**2**)]-Cl, ^{106}Pd).

*2.2.2. [Pd(**2H**)Cl]PF_6 (Pd2B)*

Brown. Yield: 70%. mp: 128–130 °C. $[\alpha]_D^{25}$ = −1.81 (c: 0.76, CH_3OH). Λ_M = 123.5 Ω^{-1} cm^2 mol^{-1}. Elemental analysis: (found: C: 44.0; H: 4.9; N: 6.3; Pd: 16.7%). Calcd. for $C_{24}H_{33}N_3ClF_6PPd$ (648.5): C: 44.4; H: 5.1; N: 6.5; Pd: 16.3. IR (KBr, cm^{-1}): ν = 840 (PF_6^-); 495 (Pd–N); 312 (Pd–Cl). ^{1}H-RMN (CD_3OD, ppm): δ = 6.91–6.83 (4H, m, H_{arom}); 6.25–6.06 (6H, m, H_{arom}); 3.52, 2.23 (2H, d, AB, J = 12.4 Hz, CH_2Ph); 3.44–3.06 (2H, m, $H_{7a,b}$); 2.97 (1H, d, AB, J = 12.9 Hz, CH'_2Ph); 2.75–2.64 (1H, m, $H_{7'a}$); 2.45–2.29 (6H, m, $H_{7'b}$, CH_2Ph, H_2, $H_{2'}$, $H_{5a,b}$); 1.31–1.29 (1H, m, H_{3a}); 0.98–0.60 (9H, m, $H_{5'a,b}$, H_{3b}, $H_{3'a,b}$, $H_{4a,b}$ $H_{4'a,b}$) ^{13}C-RMN (CD_3OD, ppm): δ = 136.07, 135.80, 135.67, 133.47, 133.10, 131.08, 130.67, 130.35, 130.13, 129.55 (C_{arom}); 74.10 (C_5); 71.18 (C_2); 65.42 (CH_2Ph); 63.91 (C′H_2Ph); 63.31 ($C_{7'}$); 62.09 ($C_{2'}$); 60.54 (C_7); 55.58 ($C_{5'}$); 24.94 ($C_{3'}$); 23.37 (C_3); 23.26 (C_4); 23.07 ($C_{4'}$). EM (*m*/*z*): 505 ([Pd(**2H**)Cl]-PF_6, ^{106}Pd).

*2.2.3. [Pd(**3**)Cl_2]CH_2Cl_2 (Pd3A)*

Green. Yield: 45%. mp: 140–142 °C. Elemental analysis: (found: C: 51.5; H: 6.0; N: 6.2; Pd: 16.2%). Calcd. for $C_{28}H_{41}N_3Cl_4Pd$ (667): C: 50.5; H: 6.1; N: 6.3; Pd: 15.9. IR (KBr, cm^{-1}): ν = 490 (Pd–N). ^{1}H-RMN ($CDCl_3$, ppm): δ = 8.17 (2H, s, H_{arom}); 7.94–7.92 (2H, m, H_{arom}); 7.56–7.24 (6H, m, H_{arom}); 5.26, 4.11 (2H, AB, J = 12.6 Hz, CH_2Ph); 4.59–4.51 (1H, m, H_5); 4.17, 3.05 (2H, d, AB, J = 12 Hz, CH_2Ph); 3.87–3.77 (3H, m, $H_{2,2''}$, $H_{5'}$); 3.62–3.68 (3H, m, H_5, $H_{7,7'}$); 2.91–2.84 (3H, m, H_7, $_{7'}$, $H_{5'}$); 2.47–2.06 (4H, m, 2$H_{4,4'}$); 1.98–1.82 (6H, m, H_8, 2$H_{3,3'}$); 1.52–1.16 (2H, m, H_9); 0.46–0.42 (3H, m, H_{10}). ^{13}C-RMN ($CDCl_3$, ppm): δ = 134.39, 132.93, 132.79, 132.70, 129.80, 129.40, 129.18, 128.82 (C_{arom}); 71,53 (C_2); 66.88 ($C_{2'}$); 63.76 (CH_2Ph); 63.17 (C_7); 61.94 (C_5); 61.57 (CH_2Ph); 61.23 ($C_{7'}$); 60.58 (C_8); 60.23 ($C_{5'}$); 30.12 (C_3); 28.78($C_{3'}$); 24.49 ($C_{4'}$); 23.29 (C_4); 13.22 (C_9); 10.83 (C_{10}). UV–vis: λ_{max} 234, 353 nm. EM (*m*/*z*): 511 ([Pd(**3**)]-[2Cl·CH_2Cl_2], ^{106}Pd).

*2.2.4. [Pd(**3**)Cl]PF_6·2CH_2Cl_2 (Pd3B)*

Black green. Yield: 53%. mp > 230 °C. $[\alpha]_D^{25}$ = −0.75 (c: 1.17, CH_3OH). Λ_M = 132.4 Ω^{-1} cm^2 mol^{-1}. Elemental analysis: (found: C: 39.8; H: 4.7; N: 4.5; Pd: 12.0%). Calcd. for $C_{29}H_{43}N_3Cl_5F_6PPd$ (861): C: 40.1; H: 4.9; N: 4.8; Pd: 12.3. IR (KBr, cm^{-1}): ν = 814 (PF_6^-); 495 (Pd–N); 307 (Pd–Cl). ^{1}H-RMN ($CDCl_3$, ppm): δ = 8.18 (1H, s, H_{arom}); 8.03 (1H, s, H_{arom}); 7.61–7.16 (8H, m, H_{arom}); 5.03 (1H, AB, J = 12.8 Hz, CH_2Ph); 4.53, 4.20 (2H, d, AB, J = 13.5 Hz, CH_2Ph); 4.36–4.29 (1H, m, H_5); 3.97–3.62 (4H, m, CH_2Ph, H_5, $H_{2,2''}$); 3.10–2.58 (6H, m, 2$H_{7,7'}$, $H_{5,5'}$); 2.56–1.97 (8H, m, $H_{4,4'}$, 2$H_{3,3'}$, H_8); 1.63–1.33 (2H, m, $H_{4,4'}$); 1.25–1.19 (2H, m, H_9); 0.48–0.46 (3H, m, H_{10}). ^{13}C-RMN ($CDCl_3$, ppm): δ = 133.00, 132.80 (C_{arom}); 132.00–128.00 (8C_{arom}); 72.85 (C_2); 66.00 ($C_{2'}$); 65.53 (CH_2Ph); 64.00 (C_7); 62.10 ($C_{7'}$); 61.83 (C_5); 61.75 (C_8); 61.65 ($C_{5'}$); 61.34 (CH_2Ph); 31.15 (C_3); 29.60 ($C_{3'}$); 24.80 (C_4); 22.60 ($C_{4'}$); 13.90 (C_9); 11.98 (C_{10}). UV–vis: λ_{max} 356 nm. EM (*m*/*z*): 547 ([Pd(**3**)Cl]-PF_6, ^{106}Pd).

*2.2.5. [Pd(**4**)Cl_2]·CH_2Cl_2 (Pd4)*

Brown. Yield: 71%. mp > 230 °C. $[\alpha]_D^{25}$ = −2.1 (c: 0.51, CH_3OH). Elemental analysis: (found: C: 49.6; H: 6.2; N: 4.9; Pd: 12.5%). Calcd. for $C_{34}H_{55}N_3Cl_4O_3Si$ (724): C: 49.3; H: 6.6; N: 5.0; Pd: 12.8. IR (KBr, cm^{-1}): ν = 1072 (Si–O); 456 (Pd–N); 304 (Pd–Cl). ^{1}H-RMN ($CDCl_3$, ppm): δ = 8.52–8.10 (2H, m, H_{arom}); 7.68–7.24 (8H, m, H_{arom}); 5.52–5.40 (1H, m, CH_2Ph); 4.68–4.50 (1H, m, H_5); 4.40–4.32 (1H, m, CH_2Ph); 4.25–4.17 (1H, m, CH_2Ph); 4.10–3.72 (2H, m, $H_{2,2''}$); 3.52–3.35 (3H, m, H_5, $H_{7,\ 7'}$); 3.15–3.08 (1H, m, CH_2Ph); 2.91–2.77 (3H, m, $H_{5'}$, $H_{7,7'}$); 2.55–2.46 (1H, m, $H_{5'}$); 2.38–2.15 (4H, m, 2$H_{4,4'}$); 2.07–1.76 (6H, m, H_8, 2$H_{3,3'}$); 1.25–1.05 (2H, m, H_9); 0.89–0.42 (3H, m, H_{10}). ^{13}C-RMN ($CDCl_3$, ppm): δ = 134.98, 134.69, 133.85, 133.44, 132.90, 129.81, 129.45 (C_{arom}); 73.11 (C_2); 72.71 ($C_{2'}$); 67.63 (CH_2Ph); 67.48 (C_7); 65.60 (C_5); 64.50 (CH_2Ph); 64.30 ($C_{7'}$); 62.82 (C_8); 61.55 ($C_{5'}$); 36.30 (C_3); 30.09 ($C_{3'}$); 25.29 (C_4); 23.95 ($C_{4'}$); 15.07 (C_9); 11.40 (C_{10}). UV–vis: λ_{max} 233, 358 nm.). EM (*m*/*z*): 708 ([Pd(**4**)Cl]–[Cl·CH_2Cl_2], ^{106}Pd).

2.3. Heterogenisation of M-complexes (Pd4-support)

2.3.1. Anchoring on mesoporous MCM-41, ITQ-2, ITQ-6 and silica: route A

The supported M-complexes (Pd4-support) were prepared as we have previously described [13,24]. Thus, a solution of metal complex bearing a triethoxysilyl group (0.5 mmol) in ethanol (2 ml) was added to a well-stirred toluene suspension (40 ml) of the inorganic support (1 g) and the mixture was stirred at 80 °C for 24 h. The solid was then filtered and Soxhlet-extracted for 7–24 h to remove the remaining non-supported complex from heterogenised

catalyst. The resulting solid was dried in *vacuum* and analysed.

Pd4-(MCM-41): Elemental analysis indicated 1.56 mass% Pd. IR (KBr, cm^{-1}): ν = 3410 (O–H); 1237 (vs, support); 1120 (C–Si); 1080 (vs, support); 450 (Pd–N). ^{13}C NMR (solid, ppm): δ = 128.86 (C_{arom}); 61.89 (C_2, C_7, C_8, C_5, CH_2Ph); 22.58 (C_4, C_9); 11.90 (C_{10}). UV–vis (solid) (nm): 357, 236.
Pd4-(ITQ-2): Elemental analysis indicated 1.28 mass% Pd. IR (KBr, cm^{-1}): ν = 3409 (O–H); 1235 (vs, support); 1120 (C–Si); 1080 (vs, support); 455 (Pd–N). ^{13}C NMR (solid, ppm): δ = 128.80 (C_{arom}); 61.91 (C_2, C_7, C_8, C_5, CH_2Ph); 29.37 (C_3); 23.06 (C_4, C_9); 10.44 (C_{10}). UV–vis (solid) (nm): 366, 238.
Pd4-(ITQ-6): Elemental analysis indicated 1.20 mass% Pd. IR (KBr, cm^{-1}): ν = 3410 (O–H); 1237 (vs, support); 1120 (C–Si); 1080 (vs, support); 450, 426 (Pd–N). ^{13}C NMR (solid, ppm): δ = 129.35 (C_{arom}); 62.86 (C_2, C_7, C_8, CH_2Ph); 55.82 (C_5); 29.61 (C_3); 21.85 (C_4); 8.99 (C_{10}). UV–vis (solid) (nm): 360, 235.
Pd4-(Sil): Elemental analysis indicated 1.53 mass% Pd. IR (KBr, cm^{-1}): ν = 3413 (O–H); 1239 (vs, support); 1120 (C–Si); 1080 (vs, support); 464 (M–N). ^{13}C NMR (solid, ppm): δ = 129.45 (C_{arom}); 62.66 (C_2, C_7, C_8, CH_2Ph); 54.61 (C_5); 29.86 (C_3); 22.58 (C_4); 10.93 (C_{10}). UV–vis (solid) (nm): 410, 229.

2.4. Catalytic experiments

The catalytic properties, in hydrogenation reactions, of the above Pd(II) and the respective Rh(I) and Ir(I) complexes were examined under conventional conditions for batch reactions in a reactor (Autoclave Engineers) of 100 ml capacity at 313 K temperature, 4 atm dihydrogen pressure and a metal:substrate molar ratio of 1/1000 (for Pd) and 1/10,000 (Rh and Ir). The results were monitored by gas chromatography using an internal standard reference. The kinetics results are shown in Tables 2 and 3 and Figs. 3 and 4.

2.4.1. Recovery and recycling of catalysts

At the end of the hydrogenation process, the mixture of reaction was filtered; the residue of zeolite-containing catalyst was washed with CH_2Cl_2 or acetonitrile to completely remove the remains of products and/or reactants and used again (Fig. 5).

Table 3
Hydrogenation of diethyl 2-benzylidenesuccinate[a]

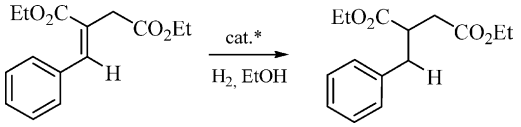

Catalyst	TOF[b,c]
Pd3	6300
Pd4-(MCM-41)	7561
Rh2	13578
Rh3	23384
Rh4-(MCM-41)	24244
Ir2	13510
Ir3	8334
Ir4-(MCM-41)	15498

[a] All reactions were performed in EtOH at 40 °C, S/C = 10,000 and 4 atm H_2.
[b] mmol substrate/mmol cat^{-1} h^{-1}.
[c] Optical yield < 10%.

3. Results and discussion

3.1. Synthesis of ligands

The ligands were prepared and well characterised following the procedure showed in Ref. [24]. All reaction steps were fine-tuned for high yield and selectivity. The preparation of diamide *N*,*N*′-bis[(*S*)-*N*-benzylprolyl]methylenamine **1**, was achieved following a modified published method starting from the easily available (L)-proline protected as the *N*-benzyl derivative, according to Scheme 1. The corresponding amine *N*,*N*′-bis{[(*S*)-1-benzylpyrrolidin-2-yl]methyl}amine **2**, was obtained by reduction of the respective amide with lithium aluminium hydride at reflux. All intermediates and final products have been obtained with a total yield of 70–80%. Amide **1** is a white solid while amine **2** was isolated as colourless oil that is stable at low temperature in an inert atmosphere. Amines **3** and **4** were obtained starting from **2** by alkylation with propyl iodide or iodopropyltriethoxysilane. The ligands were characterised unequivocally by mass spectrometry,

Table 2
TOF[a] values for the hydrogenation of olefins with palladium catalysts[b,c]

Catalyst	Diethyl itaconate	Diethyl 2-benzylidene succinate	Diethyl 2-naphthylidene succinate
Pd3	5050	1300	320
Pd4-(MCM-41)	5232	2561	457
Pd4-(ITQ-2)	5181	3541	597
Pd4-(ITQ-6)	4854	3070	551
Pd4-(Sil)	5046	1285	322

[a] mmol substrate; mmol cat^{-1} h^{-1}.
[b] All reactions were performed in EtOH at 40 °C, S/C = 10,000 and 4 atm H_2.
[c] Optical yield < 10%.

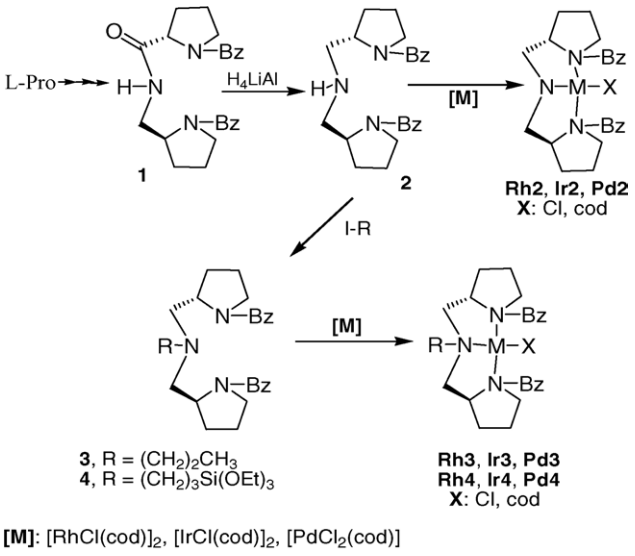

Scheme 1. Synthesis of ligands and complexes.

IR and ^{1}H, ^{13}C NMR spectroscopy and gave satisfactory elemental analyses. Mass spectrometry shows the highest ions at *m*/*z* 364, 406 and 567 that corresponds to the molecular weights of compounds **2**–**4**, respectively. The ^{1}H and ^{13}C NMR spectra obtained are in agreement with those expected for these triaza ligands. The ligands have two optically active centres; both have the *S* absolute configuration.

3.2. Preparation of complexes

Palladium complexes (Pd2–4) were prepared starting from monomeric [$PdCl_2$(cod)] and treating it with an equimolar amount of the corresponding multitopic ligands in presence of $AgPF_6$. The reaction of *N*,*N*′-bis{[(*S*)-1-benzylpyrrolidin-2-yl]methyl}amine, **2**, with [$PdCl_2$(cod)] also provided traces of the neutral M-complex, [Pd(*N*, *N*′-bis{[(*S*)-1-benzylpyrrolidin-2-yl]methyl}amine-1)Cl] (Pd2A) as a black solid by-product of the reaction, which present the ligand as a deprotonated anionic species; starting from iridium compounds the neutral species was detected as main product. The complexes were isolated by precipitation from diethyl ether as microcrystalline air stable solids. Elemental analysis of C, H, N and metal is consistent with the proposed stoichiometry. Mass spectrometry (ESI-MS and APCI-MS with positive mode) indicated a monomeric formula in accordance with the results of IR and NMR studies. The complexes have their highest ions at *m*/*z* values corresponding to the loss of F^-, and PF_6^- in the molecular species.

The IR spectrum of the mononuclear Pd2A complex does not show the expected ν(N–H) and ν(P–F) bands. In the Pd–amine complexes Pd3A, Pd-4 the ^{13}C NMR signals show only small chemical shift differences compared with the free ligand and band due to ν(P–F) was not observed.

Electronic absorption spectra of the complexes, measured between 800 and 200 nm, show a clear maximum at ca. 300 nm (ε = 6000–8000) and one shoulder at ca. 400 nm (ε = 1500–2000). Taking into account their energy position and intensity the bands at 400 nm could be assigned [25] to d–d transitions localised on the metal ion. At shorter wavelengths the bands at 300 nm may be assigned to the M → ligand charge transfer transition and intra-ligand transitions. The conductivity data suggest 1:1 electrolytes for all cationic complexes.

3.3. Heterogenisation of complexes

The solids employed in the present study as supports of the active chiral complexes were mesoporous silica such as MCM-41, ITQ-2 and ITQ-6 delaminated zeolites, amorphous silica (see characteristics in Table 1) and SBA-15. With respect to the supports, both silica and MCM-41 are short range amorphous materials containing a large number of silanol groups available for grafting. In the case of MCM-41, however, the material presents a long range ordering of hexagonal symmetry with regular monodirectional channels of 3.5 nm diameter. On the other hand, ITQ-6 and ITQ-2 delaminated zeolites present both, short and long range order, together with a large-well structured external surface (see Fig. 2a and b, respectively) in which the silanol groups act as grafting centres. However, there are structural differences between the two delaminated zeolites. Indeed, in the case of the ITQ-2 there are ‘‘cup-like’’ apertures to the external surface with ∼0.8 nm × 0.8 nm dimensions, while in the case of the ITQ-6 these ‘‘cups’’ are less deep (∼0.3 nm). In a previous work and by a molecular dynamics study, we have shown [26] that there is a minimum of potential energy in the void space of the ‘‘cups’’, in which the molecules have a high tendency to adsorb. Taking this into account and the fact that the structured silanols are located at the borders of those ‘‘cups’’ (see Fig. 2), one can envisage an structural model analogous to that presented by Breslow and Graff [27,28] for cyclodextrines, in which the grafted organometallic site is located at the border of the cyclodextrine ‘‘cup’’. In our case, the metal complex will be located at the border of the inorganic silicate cups. Then, one may expect that the reactant adsorbed in the ‘‘cup’’ of the delaminated zeolite, will react there with the catalyst located at the border. If this model is correct, we should expect an increase in the concentration of reactants close to the catalytic active site, with the corresponding increase in reaction rate.

The heterogenisation of homogeneous catalysts is a field of continuing interest: indeed, although some of these organometallic complexes exhibit remarkable catalytic properties (activities and selectivity) they are difficult to separate, intact, from the reaction medium. Thus, unless the activity of the homogeneous catalysts is exceptionally high, their heterogenisation is still currently and economical, but also a toxicological and environmental challenge. We have

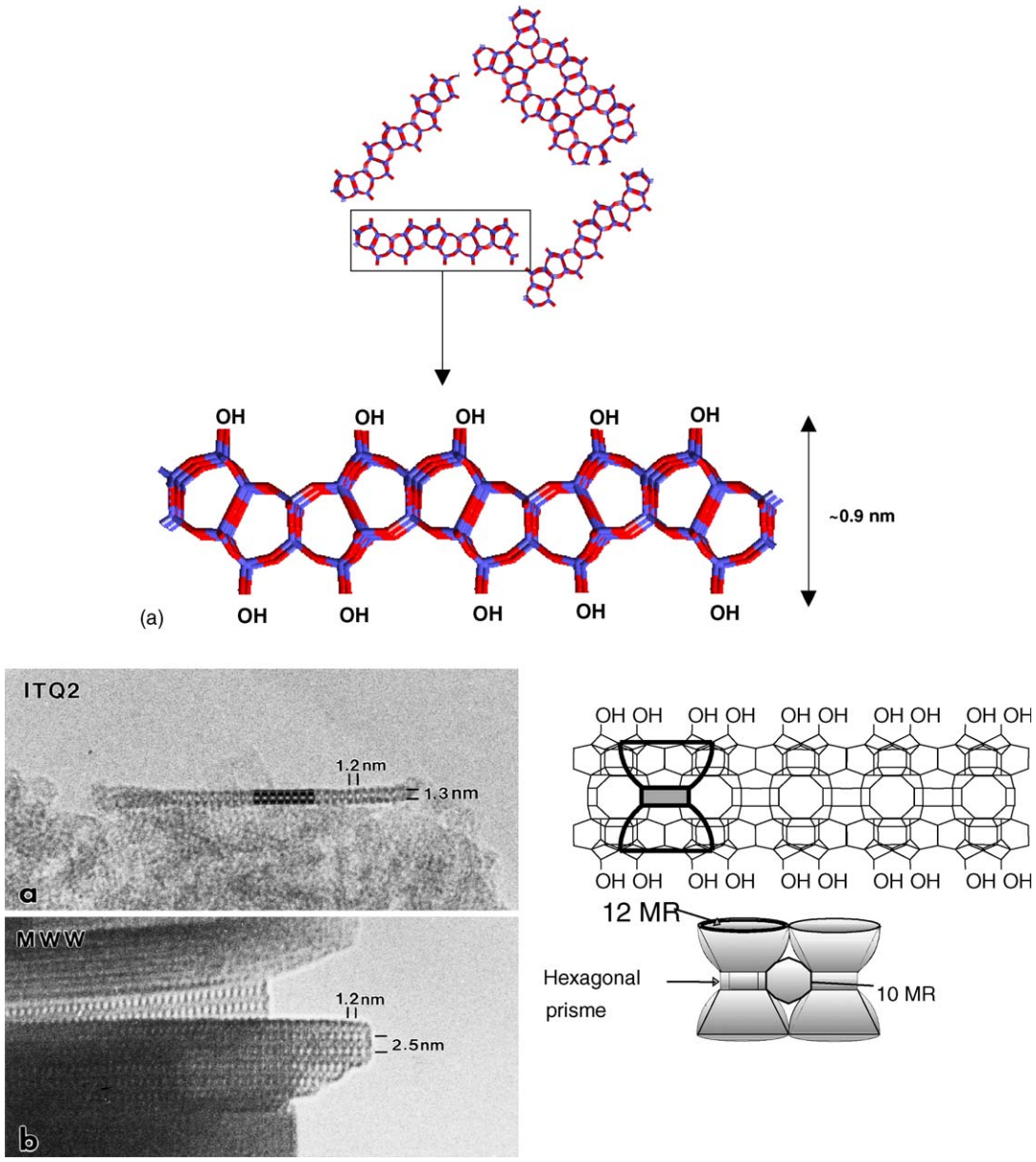

Fig. 2. (a) Structure of ITQ-6 as an ideal single layer of a delaminated ferrierite zeolite. (b) Structure of ITQ-2 as an ideal single layer of a MWW zeolite structure.

considered one strategy for heterogenisation, which preserves as much as possible the co-ordination sphere of the metal. This is achieved: by anchoring the homogeneous catalyst to an inorganic support (MCM-41, ITQ-2, ITQ-6 and silica) via covalent bonds between the solid (silanol groups –Si–OH) and one ligand that have appropriate groups ($-Si(OEt)_3$) at a position remote to the metal centre (Scheme 2A). Preparations of heterogenised materials of complexes bearing a triethoxysilylpropyl group were carried out, by controlled hydrolysis of Si–OEt bonds and reaction with the free silanol (Si–OH) on the surface of support. The resulting catalytic material is very stable and the species are covalently bonded to the surface showing only minor frequency shifts from those of the corresponding ''neat'' complex, as confirmed by IR and UV–vis spectroscopy. The elemental analysis of C, H, N and metal also confirm the metal/ligand (1:1) stoichiometry. It is unlikely that the nature of the complex is substantially altered under the relatively mild conditions of the anchoring reaction [29]. Thermogravimetric analysis shows that the total weight loss is associated with the metal complex content corresponding to composition of the organic ligands. The loading of metal was always ca. ~1–2% (±0.1%) measured by atomic absorption of metal of the digested samples. These values have been used for calculating the ratio catalyst/substrate in the reaction tests. IR and electronic spectra (diffuse reflectance) of heterogenised complexes are coincident with that recorded for homogeneous complexes. The IR spectra

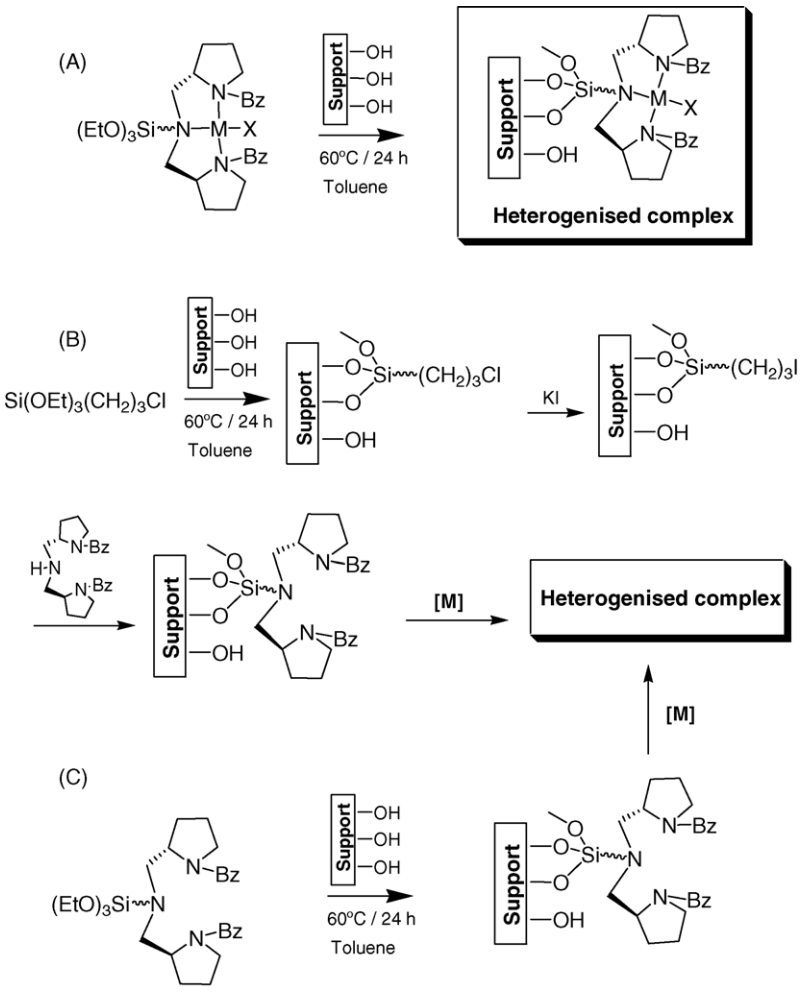

Scheme 2. Heterogenisation by covalent bond (tethering).

of the zeolite-supported catalyst show bands that correspond to the complexes and support. Peaks due to the support dominate the spectra. These include the O–H vibration in the range 3700–3300 cm^{-1}. Some of the bands characteristic of the complexes could be, however, distinguished. Major framework bands appear around 1140, 1040, 960, 785 and 740 cm^{-1}. Vibrational bands due to P–F, C–N appear around 840 and 450 cm^{-1}, respectively, broadly similar to those of the neat complex. The UV–vis electronic spectra data are given in experimental section. The band maximum is not significantly altered on zeolite heterogenised complex. The positions and relative intensities of these bands are similar to those of the free complexes.

Another alternative route was shown in Scheme 2B that consists on anchoring of iodopropyltriethoxysilane to the support (SBA-15) or by introducing a chloropropyltriethoxysilane moiety in support preparation and halogen exchange with iodide. Alkylation of amine **2** with the halide heterogenised material gives supported amines which react with the starting metal complex and M-(support) complex was obtained with similar spectroscopical characteristics that those obtained by route A.

Also, we have obtained the supported complexes by anchoring the ligand to the support (Scheme 2C) and reaction of this previously heterogenised ligand with the starting complex to give the respective heterogenised complex. These products show analytical and spectroscopical properties similar to that obtained via route A.

3.4. Catalytic experiments

3.4.1. Hydrogenation of alkenes

The use of complexes with triaza ligands is an attractive approach for the catalytic hydrogenation of alkenes as diethyl itaconate, diethyl 2-benzylidenesuccinate and diethyl 2-naphthylidenesuccinate. The reactions were carried out under standard conditions (EtOH as the solvent, 4 atm hydrogen pressure and 40 °C). The hydrogenation was

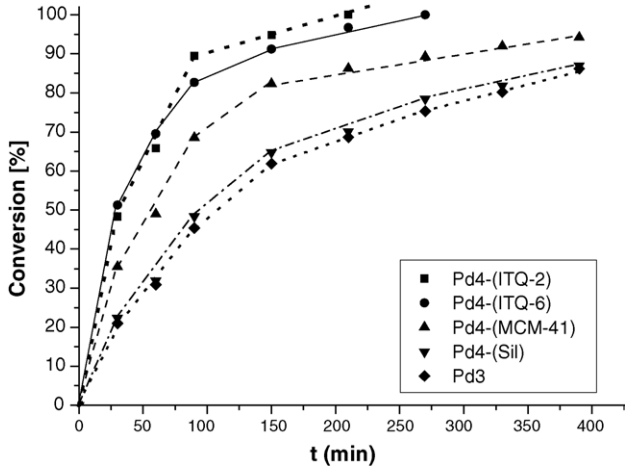

Fig. 3. Effect of the support on the kinetic profile for the catalytic hydrogenation of 2-naphthylidene succinate.

carried to explore the possibilities of recovering the catalysts, the influence of the nature of the support and the comparison of the activity and stability of supported catalysts with their homogeneous counterpart. In the present study, the order of reactivity may be explained on the basis of the steric factors. As can be seen in Fig. 3 and Table 2 when the complexes were supported on amorphous silica, the TOF did not decrease but remains practically the same than when in homogeneous phase. Interestingly, the activity of the catalyst increases when supported on the mesoporous molecular sieve MCM-41. The increase in activity is even higher in the case of the delaminated zeolitic materials whose surface is formed by accessible cups in which the reactant will be concentrated by adsorption [30–33]. In this case, the activity when grafted on ITQ-2 is almost double than for the unsupported homogeneous catalyst. The results show the benefit of the high surface area, accessibility and adsorption properties of MCM-41, ITQ-2 and ITQ-6. Furthermore, these structured materials allow modifications of the surface that can further enhance the catalytic performance of the hybrid organic–inorganic catalysts.

Triaza metal complexes were also evaluated as catalysts in the hydrogenation of diethyl 2-benzylidene succinate to investigate the potential of ligands **2**–**4** for catalysis (Table 3; Fig. 4). In the presence of 0.1 mol% of catalysts in ethanol at 313 K under a pressure of 4 bar H_2, the substrate was fully converted to corresponding saturated di-ester in 60 min. The results of these studies reveal that catalysts are very effective for this transformation affording the product with higher rate and comparable enantioselectivity to that achieved with the analogous tetraaza derivatives [8]. Fig. 4 presents the different performance that the catalysts show for hydrogenation of diethyl 2-benzylidene succinate. As can be seen Pd4-(MCM-41) shows similar performance than the respective rhodium or iridium catalysts. The change of substituents on primary amine nitrogen plays a significative role on activity that increases when moving from hydrogen to propyl group. When transition metal complexes have been supported on carriers such as polymers or silica, etc., it is generally accepted that a moderate to strong reduction in the reactivity has been observed; however, in our case the turnover numbers for hydrogenation increase indicating the co-operative effect of the support.

Soluble complexes could be used only once, because of they deteriorate completely by the end of the first catalytic run, with Pd(0) deposition; supported-complexes could be recovered for recycling, and reused retaining most of their catalytic activity. After each cycle, the liquid phase that was separated from the reaction mixture was examined for catalytic activity in the hydrogenation of alkenes under the same conditions used with the solid catalyst. The results show that the liquid phases are inactive for hydrogenation. Moreover, atomic emission analyses did not detect metal in the liquid phases from the first, second and third cycles. Based on the lower detection limit of the instrument, the amount of metal leaching into the liquid phases must be less than 0.2% of the metal on the catalyst.

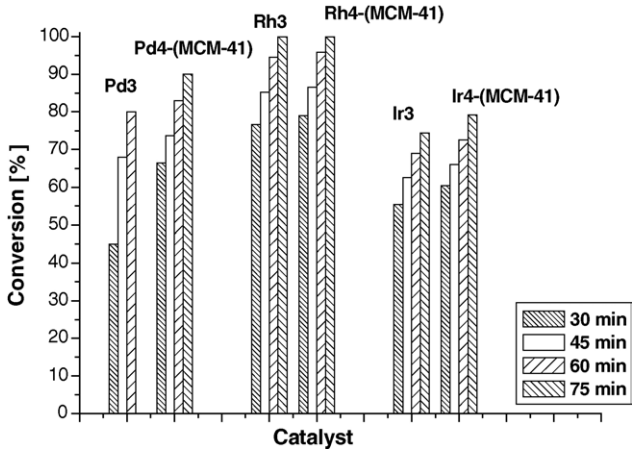

Fig. 4. Kinetic profile for the hydrogenation of diethyl 2-benzylidene succinate.

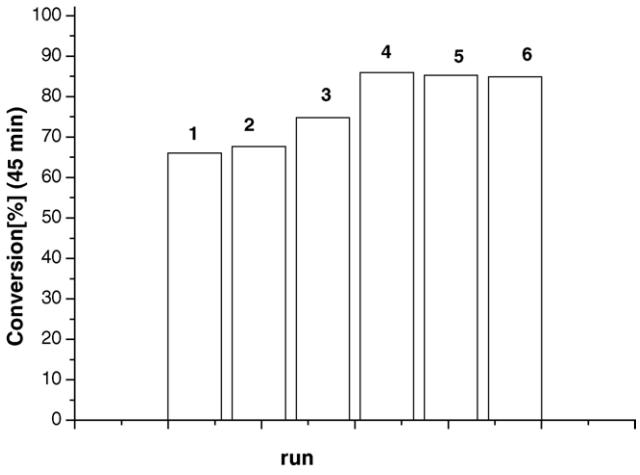

Fig. 5. Recycling experiments for the hydrogenation of diethyl 2-benzylidene succinate with Rh4-(SBA-15).

The possibility for the recovery and reuse of the heterogeneous catalyst was explored thoroughly with Rh4-(SBA-15) (Fig. 5). The results obtained indicate that after the first reaction, the recovered catalyst does not show a significant degree of leaching of rhodium (metal loss $<2\%$ measured by atomic absorption of digested samples). We have carried out the heterogeneous asymmetric hydrogenation of olefins until completion, filtered and washed the heterogenised catalyst, then added fresh substrate, and solvent without further addition of catalyst, for several consecutive experiments and have found that both yield and activity are retained. On the other hand, the filtrate has been used in a new reaction and was not found to catalyse hydrogenation.

The spectral data for recovered material are essentially the same before and after the hydrogenation reaction.

4. Conclusion

We have shown that it is possible to boost the activity of an organometallic catalyst by using an adequate support. We have seen that by using mesostructured silicates and delaminated zeolites as carriers, both with very high surface areas and accessibility to reactants, together with high adsorption capacity, the activity of the grafted Pd, Rh and Ir triaza complex for the hydrogenation of alkenes is higher than with the homogeneous counterpart or when grafted on amorphous silica. The stability of the catalysts was excellent and no deactivation was observed.

Acknowledgement

Financial support by the Dirección General de Investigación Científica y Técnica of Spain (Project MAT2003-07945-C02-02) is gratefully acknowledged.

References

[1] A. Togni, L. Venanzi, Angew. Chem. Int. Ed. Engl. 33 (1994) 497.
[2] F. Fache, E. Schulz, M. Lorraine Tommasino, M. Lemaire, Chem. Rev. 100 (2000) 2159.
[3] M.H. Fonseca, B. König, Adv. Synth. Catal. 345 (2003) 1173.
[4] F. Fache, B. Dunjic, P. Gámez, M. Lemaire, Top. Catal. 4 (1997) 201.
[5] G. Jannes, V. Dubois (Eds.), Chiral Reactions in Heterogenous Catalysis, Plenum Press, New York, London, 1995.
[6] D.E. Vos, I.F.K. Vankelecom, P.A. Jacobs (Eds.), Chiral Catalyst Inmobilization and Recycling, Wiley-VCH, Weinheim, 2000.
[7] M.J. Alcón, E. Gutiérrez-Puebla, M. Iglesias, M.A. Monge, F. Sánchez, Inorg. Chim. Acta 306 (2000) 116.
[8] M.J. Alcón, M. Iglesias, F. Sánchez, J. Organomet. Chem. 601 (2000) 284.
[9] M.J. Alcón, M. Iglesias, F. Sánchez, J. Organomet. Chem. 634 (2001) 25.
[10] M.J. Alcón, M. Iglesias, F. Sánchez, Inorg. Chim. Acta 333 (2002) 83.
[11] M.J. Alcón, A. Corma, M. Iglesias, F. Sánchez, J. Organomet. Chem. 655 (2002) 134.
[12] M.J. Alcón, A. Corma, M. Iglesias, F. Sánchez, J. Mol. Catal. A: Chem. 178 (2002) 253.
[13] M.J. Alcón, A. Corma, M. Iglesias, F. Sánchez, J. Mol. Catal. A: Chem. 194 (2003) 137.
[14] E. Miranda, F. Sánchez, J. Sanz, M.I. Martínez-Castro, J. High Resolut. Chromatogr. 21 (1998) 225.
[15] C.T. Kresge, M.E. Leonowicz, W.J. Roth, J.C. Vartuli, J.S. Beck, Nature 359 (1992) 710.
[16] J.S. Beck, W.J. Roth, M.E. Leonowicz, C.T. Kresge, K.D. Schmitt, C.T.-W. Chu, K.H. Olson, E. Sheppard, S.B. McCullen, J.B. Higgins, J.L. Schlenk, J. Am. Chem. Soc. 114 (1992) 10834.
[17] A. Corma, V. Fornés, J.M. Guil, S. Pergher, T.L.M. Maesen, J.G. Buglass, Microporous Mesoporous Mater. 38 (2000) 301.
[18] A. Corma, V. Fornés, S.B. Pergher, Nature 396 (1998) 353.
[19] A. Corma, V. Fornés, J. Martínez-Triguero, S.B. Pergher, J. Catal. 186 (1999) 57.
[20] A. Corma, U. Diaz, M.E. Domine, V. Fornés, Angew. Chem. Int. 39 (2000) 1499.
[21] A. Corma, U. Diaz, M.E. Domine, V. Fornés, J. Chem. Soc.,Chem. Commun. (2000) 137.
[22] D.Y. Zhao, J.L. Feng, Q.S. Huo, N. Melosh, G.H. Fredrickson, B.F. Chmelka, G.D. Stucky, Science 279 (1998) 548.
[23] K. Ishihara, Y. Karumi, S. Kondo, H. Yamamoto, J. Org. Chem. 63 (1998) 5692.
[24] C. González-Arellano, A. Corma, M. Iglesias, F. Sánchez, Inorg. Chim. Acta 357 (2004) 3071–3078.
[25] R.D. Peacock, B. Steward, Coord. Chem. Rev. 46 (1982) 129.
[26] G. Sastre, C.R.A. Catlow, A. Corma, J. Phys. Chem. B 103 (1999) 5187.
[27] R. Breslow, A. Graff, J. Am. Chem. Soc. 115 (1993) 10988.
[28] R. Breslow, Acc. Chem. Res. 29 (1991) 317.
[29] L.L. Murrell, in: J.J. Burton, R.L. Garten (Eds.), Advanced Materials in Catalysis, Academic Press, NY, 1977 (Chapter 8).
[30] A. Corma, V. Fornés, S.B. Pergher, Nature 396 (1998) 353.
[31] A. Corma, V. Fornés, J. Martínez-Triguero, S.B. Pergher, J. Catal. 186 (1999) 57.
[32] A. Corma, U. Díaz, M.E. Domine, V. Fornés, Angew. Chem. Int. Ed. 39 (2000) 1499.
[33] A. Corma, U. Diaz, M.E. Domine, V. Fornés, J. Chem. Soc. Chem. Commun. (2000) 137.